

Accuracy of the master-event and double-difference locations: synthetic tests and application to seismicity in West Bohemia, Czech Republic

Fateh Bouchaala · Václav Vavryčuk ·
Tomáš Fischer

Received: 20 September 2012 / Accepted: 20 February 2013 / Published online: 15 March 2013
© Springer Science+Business Media Dordrecht 2013

Abstract The relative locations of earthquake hypocentres determined with the master-event (ME) or the double-difference (DD) methods are more accurate and less dispersive compared to the absolute locations. In this paper, we conduct synthetic tests to assess the accuracy of the ME and DD location methods, to study the effects of the control parameters on the locations and possible distortions of the foci geometry. The results indicate that the DD locations are, in general, more accurate than the ME locations and perform significantly better for large earthquake clusters due to their independence of the master event position. The location precision, however, strongly depends on the control parameters used. If the control parameters are optimally chosen, the location errors can be considerably reduced. Moreover, it is proved that no distortion such as artificial clustering of foci is introduced if relative locations are used. Finally, the efficiency of both location methods is exemplified on locations of swarm micro-earthquakes that occurred in the West Bohemia region, Czech Republic, in order to reveal a detailed geometry of the active fault zone.

Keywords Earthquakes · Earthquake swarm · Faults · Locations · Seismicity

1 Introduction

The classical absolute methods for location of earthquake hypocentres are based on minimizing the residuals between the predicted and observed travel times from the source to the stations. The accuracy of these methods is controlled by errors in arrival times and by inaccuracies in the velocity model (Pavlis 1986). The errors introduced by the velocity model can be considerably minimized using the relative location methods such as the master-event (ME) method or the double-difference (DD) method. The ME method is based on minimizing the residuals between the predicted and observed differential times of the processed event and the master event (Zollo et al. 1995; Havskov and Ottemoller 2010). On the contrary, the DD method minimizes the residuals between the predicted and observed differential times of neighbouring events (Waldhauser and Ellsworth 2000). These methods were successfully applied to numerous studies of various seismically active areas producing more focused patterns of seismicity and more detailed shapes and orientations of active faults (Stoddard and Woods 1990; Zollo et al. 1995; Waldhauser and Ellsworth 2000, 2002) than the absolute location methods.

The properties of the DD and ME methods have also been studied numerically on synthetic data, in

F. Bouchaala · V. Vavryčuk (✉) · T. Fischer
Institute of Geophysics, Academy of Sciences,
Boční II/1401, 14100 Prague 4, Czech Republic
e-mail: vv@ig.cas.cz

T. Fischer
Faculty of Science, Charles University in Prague,
Albertov 6, Prague 2, Czech Republic

order to test their sensitivity to uncertainties present in the input data (i.e. in the velocity model and in arrival times). For example, Michelini and Lomax (2004) applied the DD method to a circular cluster of foci and showed that an inappropriate choice of the velocity model combined with unbalanced source-receiver distributions can lead to a significant distortion of the cluster and a bias in the relative hypocentre positions. Lin and Shearer (2005) located a cluster of foci by three relative methods: the DD method, the hypocentroidal decomposition method (Jordan and Sverdrup 1981) and the source-specific station term method (Richards-Dinger and Shearer 2000). They showed that the three methods produced very similar results for a compact cluster and almost the same errors due to the uncertainties in the model and data. Jones et al. (2008) showed that, in addition to uncertainties in the arrival times and in the isotropic velocity model, the DD locations can be affected by neglecting or underestimating the seismic anisotropy.

In this paper, we focus on a thorough comparison of the efficiency and accuracy of the ME and DD methods. We perform a series of synthetic tests regarding the optimal choice of the parameters affecting the location results and study the possible distortion of the focal zone introduced by the methods. We also compare the DD and ME locations in terms of their sensitivity to errors in arrival times and inaccurate velocity models. After synthetic tests, we exemplify the properties of the ME and DD methods on real observations of the seismicity in West Bohemia, Czech Republic. This region is characteristic and well known for the reoccurrence of earthquake swarms, and the configuration of the seismic network and geometry of the focal zone are suitable for calculating highly accurate relative locations.

2 Location methods

2.1 Absolute locations

The absolute location methods aim to minimize the differences between the observed and predicted travel times at stations for a single event (e.g. Herrmann 1979). The procedure is basically non-linear and is usually linearized and solved using the least-squares method (Menke 1989; Lay and Wallace 1995). In this method, a truncated Taylor series expansion is used to relate

linearly the travel-time residual r_k^i between the observed and calculated travel times of event i recorded by station k to the error in its location and in its origin time, $\Delta \mathbf{p}^i = (\Delta x^i, \Delta y^i, \Delta z^i, \Delta t_0^i)$, by the relation:

$$\frac{\partial t_k^i}{\partial \mathbf{p}} \Delta \mathbf{p}^i = r_k^i. \quad (1)$$

Vector $\Delta \mathbf{p}^i$ represents the variations in the hypocentre parameters, which would minimize residual r_k^i . Usually, the linearized inversion converges rapidly unless the stations are badly configured or the initial location is very far away from the optimum solution. The other possibility is to keep the non-linearity of the problem and apply non-linear solvers or grid search over all possible locations to find the minimum of the sum of the squared residuals,

$$e^i = \sum_{k=1}^N (r_k^i)^2 = \min \quad (2)$$

where N is the total number of observations.

The accuracy of the final solution obtained using the minimization procedure is affected by two main factors: (1) by uncertainties in the velocity model along the ray paths and (2) by the errors in arrival times. While the former can be separated into the uncertainties of the velocity structure of the focal zone, the intermediate medium and the near station effects, the latter includes the random picking errors and errors in the time base of the seismic stations.

2.2 Master-event locations

To compensate for the systematic errors in the arrival times and for the uncertainties in the velocity structure between the focal zone and stations, relative location methods are used. A classical approach is represented by the ME method (e.g. Stoddard and Woods 1990; Zollo et al. 1995), which minimizes the differences between the observed and calculated differential travel times of the phase k observed for the located event i and the master event:

$$dr_k^i = (t_k^i - t_k^{\text{ME}})^{\text{obs}} - (t_k^i - t_k^{\text{ME}})^{\text{cal}}, \quad (3)$$

$$e^i = \sum_{k=1}^N (dr_k^i)^2 = \min \quad (4)$$

where superscript ‘obs’ stands for the observed quantities, superscript ‘cal’ for the calculated quantities, i identifies the event and ME the master.

It is required that the master event be recorded at a large number of stations, and to be located optimally in the centre of the cluster of events to ensure approximately parallel ray paths of the master and located events to the stations. Additionally, the extent of the located cluster should be small compared to the epicentral distances. This limits the use of the ME method to earthquake clusters much smaller than the seismic network aperture, the event-station distance and the scale length of the velocity heterogeneities. Given these conditions, the ray paths between the sources and the individual stations are similar for almost the entire ray, with the main deviation occurring in the source region (Frèchet 1985; Got et al. 1994). With this ray geometry, the differences in the travel times can be attributed with high accuracy to the spatial offset between the events.

Some examples of the successful application of the ME method include the relocations of earthquakes in the northern part of the Gorda block (Stoddard and Woods 1990) or the identification of active faults in the upper crust of northern Switzerland (Deichmann and Garcia-Fernandez 1992). The ME method was also successfully applied to mining-induced microseismic events after excavation (Gibowicz and Kijko 1994).

2.3 Double-difference locations

The DD method (Waldhauser and Ellsworth 2000) overcomes the ME constraints by minimizing the differences between the observed and calculated differential travel times of any two events i and j recorded at the same station k :

$$d\tau_k^{ij} = (t_k^i - t_k^j)^{\text{obs}} - (t_k^i - t_k^j)^{\text{cal}} \tag{5}$$

This way, the ME requirement that the located and the master events be recorded at the same stations and the distance between the events be small enough applies to individual event pairs. This provides the opportunity precisely locating the earthquakes that are spread in space and recorded at different stations. With this method, it is possible to use both absolute travel times and also waveform cross-correlation differential

times to improve the precision of the hypocentre locations.

In the DD method, pairs containing two neighbouring events are created. The events are located relative to each other. If we combine Eq. 5 for M event pairs observed at N stations, we get a system of linear equations of the form

$$\mathbf{WGc} = \mathbf{Wd} \tag{6}$$

where \mathbf{G} is the $N \times 4M$ matrix of the partial derivatives of the double differences with respect to the hypocentral parameters, \mathbf{d} is the N vector containing the double differences, \mathbf{c} is the $4M$ vector containing the perturbations of the hypocentral parameters we wish to determine, and \mathbf{W} is the diagonal matrix of weights. If one event is poorly linked to the other events, then matrix \mathbf{G} is ill conditioned and Eq. 6 becomes numerically unstable. The instability is resolved by damping the solution by factor λ .

The DD method is widely used to locate earthquake hypocentres with high precision. It was applied for the first time by Waldhauser and Ellsworth (2000) to two clusters of earthquakes located on the northern Hayward fault, California. The DD locations showed less dispersion and gave more details of the fault. After that, numerous successful applications of the DD method were published: for example, the locations of aftershocks in the Çınarcık basin in Turkey, associated with the 1999 Izmit earthquake Mw 7.4 (Bulut and Aktar 2007) or the precise locations of the aftershocks of the 2003 Tecoman (Colima, Mexico) earthquake (Andrews et al. 2011).

2.4 Cross-correlation of waveforms

In addition to the above advantages of the ME and DD methods, the precision of the hypocentre locations can further be improved by including differential travel times computed using cross-correlations. The cross-correlation measures the similarity of two waveforms $x(t)$ and $y(t)$ as a function of time lag τ :

$$C_{xy}(\tau) = x(t) \otimes y(t) = \int_{-\infty}^{+\infty} x(t)y(t + \tau) dt \tag{7}$$

where ‘ \otimes ’ symbolizes the correlation operator.

If two events forming a pair have close foci, the waveforms should be similar because they are affected by the medium in the same way. In this case, the differential times between the events can be efficiently computed by the waveform cross-correlation. The cross-correlation differential times are in general highly accurate. They are less sensitive to the signal-to-noise ratio because they are calculated as time shifts between the whole waveforms including cases when the actual onsets are hidden in noise. Moreover, they can principally be determined with errors even less than the sampling interval if the waveforms are oversampled before being cross-correlated.

2.5 Location accuracy

The ME and DD methods give precise relative locations and provide focused images of fault geometry. As regards the absolute locations, it is commonly assumed that the relative methods cannot improve their accuracy because the differential travel times depend on the distances between the located events only. However, Menke and Schaff (2004) showed with synthetic tests that the absolute locations can, in principle, be determined even by using the DD travel times. Their results show that the absolute locations, computed from the DD differential times, have errors comparable in magnitude, or even smaller than the absolute methods. The improvement arises from the same reasons why the DD method yields superior relative locations: (1) the high accuracy of the differential times computed by cross-correlations, and (2) the smaller sensitivity of the differential times to systematic station-dependent errors and to the inaccuracies in the velocity model between the foci and stations than the absolute travel times.

Similarly to other studies, we distinguish between the absolute location errors, which are related to the term ‘location accuracy’, and the relative location errors, which are related to the term ‘location precision’. The relative location errors are understood to be errors of event location relative to the other events in the cluster.

3 Synthetic tests

In this section, we perform a series of synthetic tests in order to exemplify the properties and the efficiency of

the ME and DD methods. We adopt a station configuration and geometry of the focal zone, which mimics observations of seismicity in West Bohemia, Czech Republic, used as an example of the real application in Sections 4 and 5. The West Bohemia region is monitored by the local seismic network WEBNET consisting of 13 three-component permanent seismic stations and 10 mobile seismic stations densely covering the region under study (see Fig. 1). The epicentral distances of stations are up to 30 km, the depth of the foci is between 7 and 11 km. The configuration of the network and the position and size of the focal zone guarantee high-quality recordings of the earthquakes. The combination of good station coverage and an extensive number of earthquakes focused in a small and compact seismic zone make the application of the ME and DD methods particularly suitable.

For testing the precision of the location methods, we create a synthetic dataset consisting of 675 regularly spaced foci at depth of 9 km. The foci are divided into nine sub-clusters, separated by distances of 50 and 30 m in the N–S and E–W directions, respectively. Neighbouring foci belonging to the same cluster are separated by 30 m in the N–S direction, by 20 m in the E–W direction and by 60 m in depth. Hence, the size of the whole cluster is about 800 m in the N–S direction, 600 m in the E–W direction and 200 m in depth (Fig. 2). The mean depth of the cluster is 9.2 km. We evaluate the location error as the distance difference between the true location and the located position.

The synthetic travel times of the P and S waves from foci to the stations are computed using a 1D layered velocity model proposed for the West Bohemia region obtained by refining the model of Málek et al. (2000). The V_p/V_s ratio is 1.70. This model is also used for the relocations, except for the cases when velocity mismodelling is tested using a homogeneous model. The initial locations of foci for the DD method are obtained by randomly perturbing the true foci, the mislocation error reaching values of up to 300 m for some events.

3.1 Master-event locations

The algorithm used for the relocation is similar to the method of Zollo et al. (1995), which is based on the minimization of the squares of the differential residuals between the located and ME events (see Eqs. 3 and 4). To find the minimum of the misfit function, a

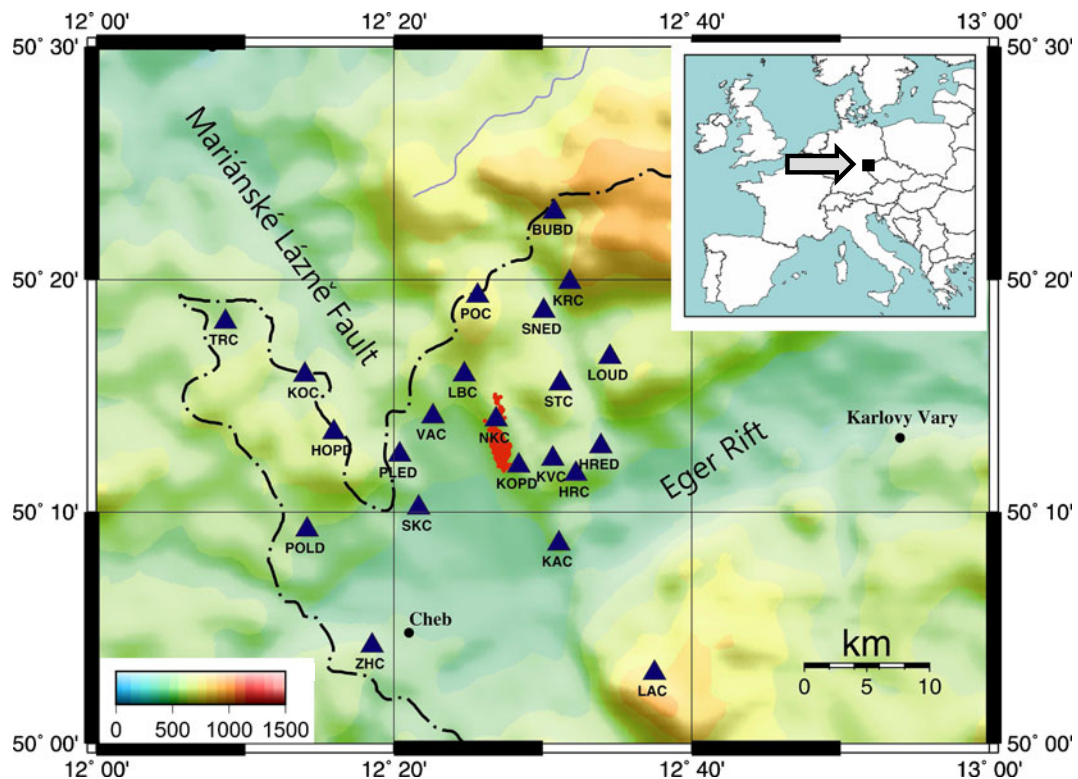


Fig. 1 The topographic map of the West Bohemia/Vogtland region. The epicentres of the 2008 swarm micro-earthquakes are marked by red circles; the WEBNET stations are marked by

blue triangles. The dashed-dotted line shows the border between the Czech Republic and Germany. The colour scale shows the surface elevation in metres

grid search in coordinate space with a gradually decreasing grid size is applied. This guarantees successful convergence of the location with no need of setting the initial location.

The main control parameter of the algorithm is the position of the master event within the located cluster. To test the sensitivity of the method to this parameter, we use three different master events: first, in the centre of the focal zone, second, between the centre and edge of the focal zone, and third, at the edge of the focal zone. True positions with no mislocation errors are used for the master events, and exact (noise-free) travel times are inverted. The results show that the average error of the locations is almost the same for the three positions of the master event: the average error is 5.58 m when the master event is positioned in the middle of the focal zone (Fig. 2), and 5.72 m when it is positioned at the edge of the focal zone. This indicates that the role of the relative position of the master event in the focal zone is minor if noise-free data are inverted. When the three ME positions are

shifted by 10 m in depth, the whole cluster also shifts the same distance in depth as the master event, and the error increases. This indicates that the shape of the structure is almost independent of the accuracy of the ME location, which affects the absolute locations only.

The sensitivity to errors of arrival times is tested by perturbing the true travel times by random noise uniformly distributed from -10 to 10 ms for the P waves and from -15 to 15 ms for the S waves. In this case, the location errors increase slightly compared to the noise-free data, the average error being 5.70 m when the master event is positioned in the centre of the focal zone, and 5.89 m when it is positioned at the edge. Nevertheless, the locations remain stable and close to the exact locations. If we increase the noise level to -15 and 15 ms for the P waves and -30 and 30 ms for the S waves, the effect of noise is more visible, especially at the hypocentral depth (Fig. 2), and the average error increases to 35.10 m.

The errors of the ME locations increase if the seismic velocity model is unknown or very approximate. This is

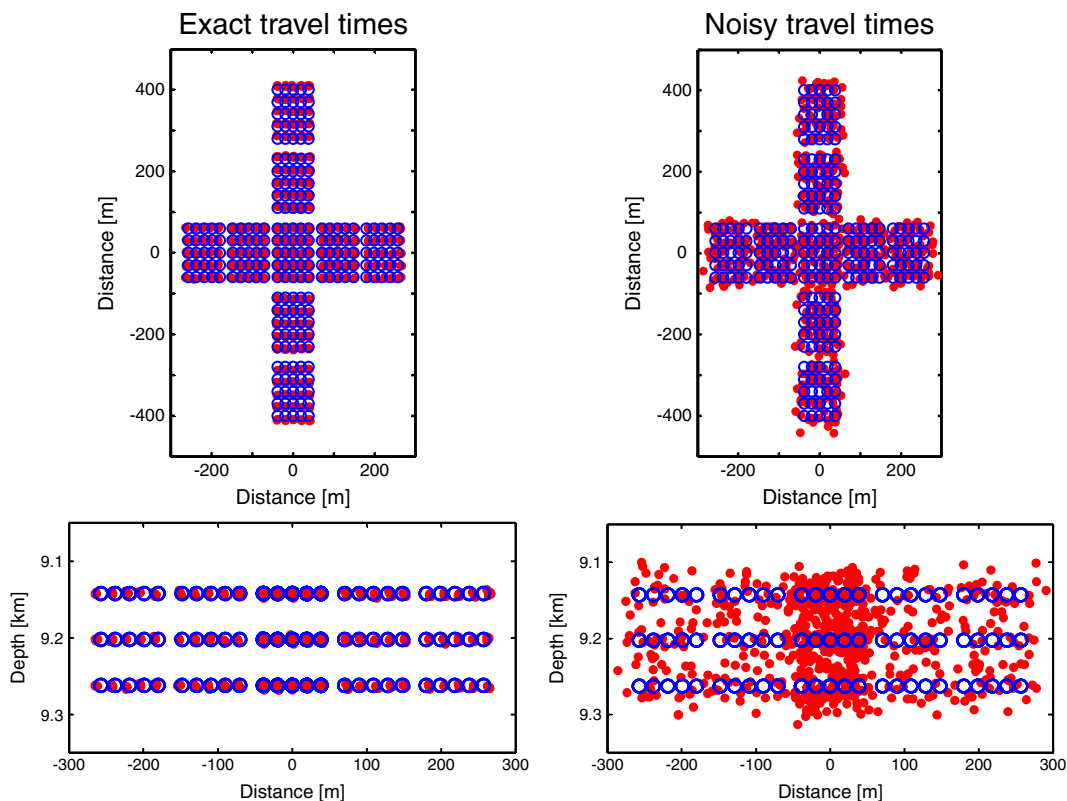


Fig. 2 Synthetic test of the master event locations (*red dots*) with the master event positioned in the centre of the focal zone for noise-free travel times (*left*) and travel times disturbed by

random noise (*right*) with maximum level of ± 15 ms for the P waves and ± 30 ms for the S waves. True locations are marked by *blue circles*

simulated by calculating the noise-free synthetic travel times in a 1D velocity model and locating in a homogeneous half-space velocity model and by using three different master events. As expected, the highest precision of locations is achieved when the master event is positioned in the centre of the focal zone: the average error is 7.76 m in this case. The lowest precision is for the master event at the edge of the focal zone, the average error being 19.70 m. This finding indicates that the role of the relative position of the master event in the focal zone is important and that the velocity mismodelling increases the location errors. The influence of the velocity mismodelling is checked also by examining the dependence of the location error on the distance from the master event (Fig. 3). It turns out that the location error increases linearly with the distances of the foci from the ME position.

Finally, we test the effect of the number of stations on location precision. We decrease gradually the number of stations from 23 to 4 and locate noise-free as

well as noisy data. The tests indicate that the errors increase only slightly by decreasing the number of stations (see Table 1 and the black curves in Fig. 4). As expected, the noisy data show several times higher location errors than the noise-free data.

3.2 Double-difference locations

The DD locations can be calculated using the HypoDD code designed and published by Waldhauser (2001). The location strategy in this code is controlled by several parameters. One of the most important parameters is the maximum separation distance (MAXSEP) between two events i and j forming one pair. This parameter controls the size of the created clusters and inversely also the number of clusters being located. Additionally, it affects the number of events excluded from the location procedure due to the small number of links to neighbouring events. The maximum number of neighbouring events is limited by the MAXNGH parameter.

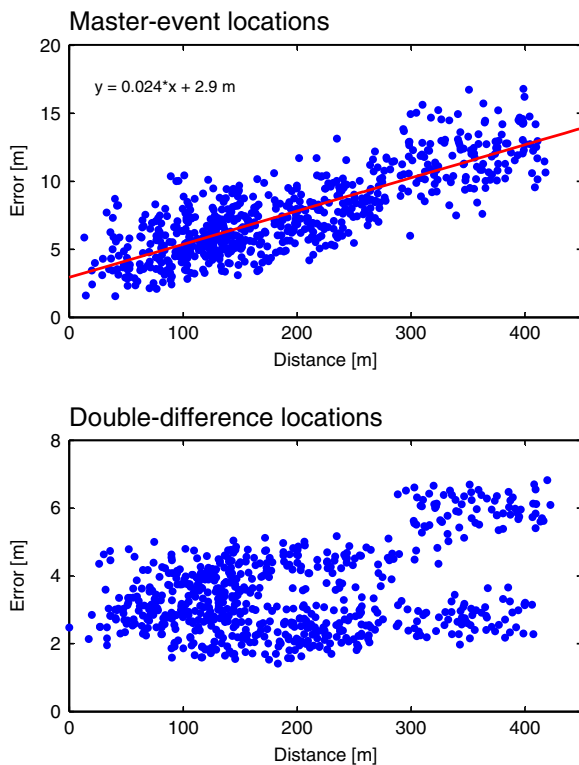


Fig. 3 The variation of the error of the master-event (*top*) and double-difference (*bottom*) locations with respect to the distance from the master-event position and from the centre of the focal zone, respectively. The *equation* and the *red line* represent the result of the linear fitting

First, we test the location accuracy in the exact 1D velocity model and for noise-free travel times. We vary the MAXSEP parameter from 20 m to 1 km, locate the events with the perturbed initial locations and compare the results with the exact locations. The most accurate locations are found for the MAXSEP value of 1 km. The lowest accuracy is achieved for the MAXSEP value of

Table 1 The master-event and double-difference average errors

Number of stations	Noise-free data		Noisy data (15 ms for P and 30 ms for S)	
	ME error (m)	DD error (m)	ME error (m)	DD error (m)
23	5.58	3.53	35.10	15.72
16	5.75	4.02	37.21	18.30
12	6.42	4.51	39.72	22.51
8	6.88	5.02	42.97	30.12
4	10.07	11.71	51.21	58.21

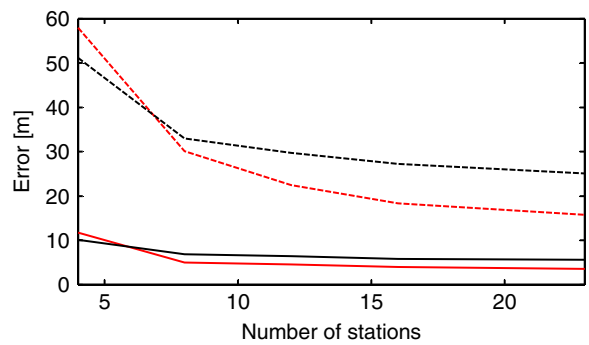


Fig. 4 The variation of the average error of the double-difference (*red colour*) and master-event (*black colour*) locations with respect to the number of stations for noise-free data (*solid line*) and for noisy data (*dashed line*)

20 m (Fig. 5). Figure 6 shows the average errors in location and travel time as a function of MAXSEP. It clearly shows that the error decreases as MAXSEP increases. This is because high values of the separation distance allow for a large number of foci pairs. The foci are then strongly linked, and the system of equations is well overdetermined. When MAXSEP becomes smaller than 70 m, the error increases considerably in our event configuration, as the data are divided into multiple clusters. The events from two different clusters are not linked and thus they are located separately. A similar tendency is observed also if the maximum number of foci pairs per event, controlled by parameter MAXNGH for MAXSEP fixed at a value of 1 km, is varied. The minimum value of MAXNGH is equal to 3, so one event can have a minimum of three foci pairs. The location errors decrease with an increasing total number of foci pairs confirming the above results. Therefore, in the following tests, we maintain the MAXSEP distance equal to 1 km and the MAXNGH equal to 50, which ensure a sufficiently large number of foci pairs.

Second, we test the location accuracy in the exact 1D velocity model and for noisy data after adding random noise uniformly distributed from -10 to 10 ms for the P waves and from -15 to 15 ms for the S waves. The tests show that the DD locations remain stable and close to the exact locations by 4.5 m on average. However, after increasing the random noise to levels from -15 to 15 ms for the P waves and from -30 to 30 ms for the S waves, the average error of locations increases to 15.70 m (Fig. 7).

Third, we tested the dependence of the location precision on the number of stations. We decreased the number of stations by decreasing the maximum

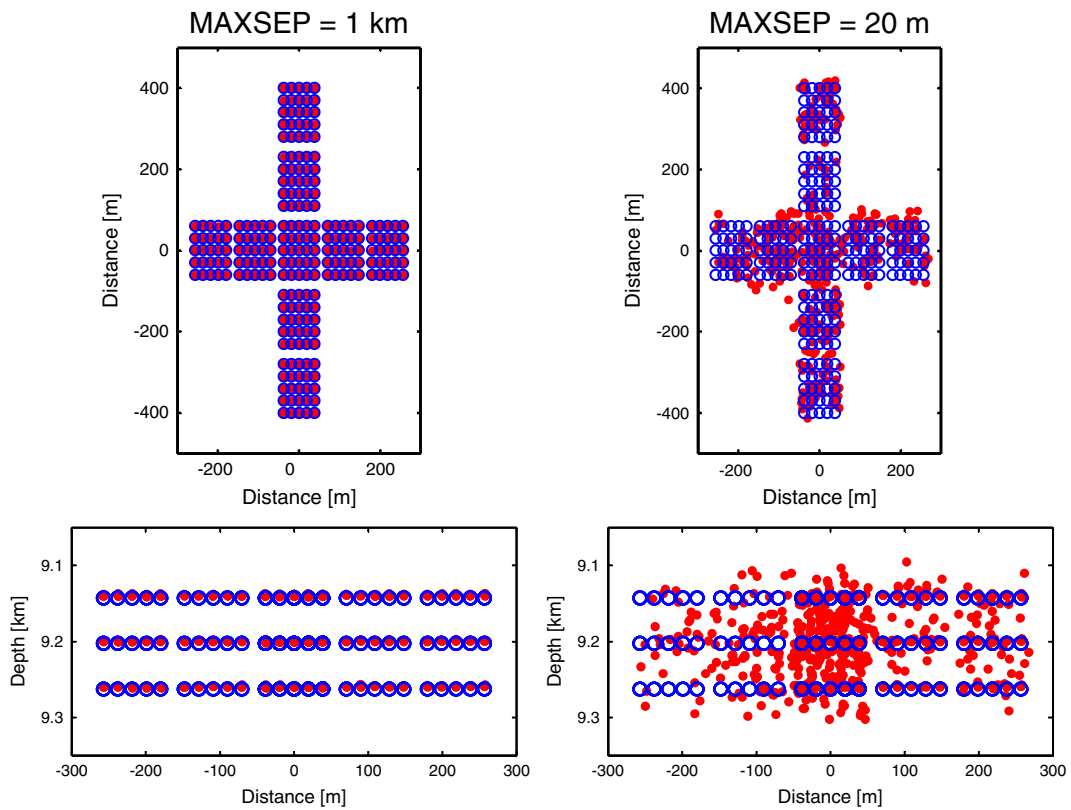


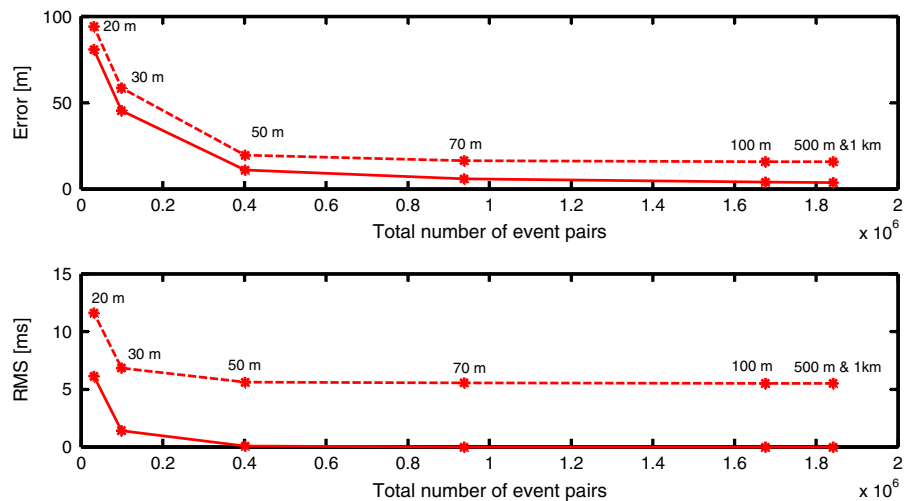
Fig. 5 Double-difference synthetic locations (*red dots*) for noise-free travel times with parameter MAXSEP set at 1 km (*left*) and at 20 m (*right*), compared to the exact locations (*blue circles*)

number of observations (MAXOBS). As expected, the error decreases if the number of stations increases (Fig. 4 and Table 1), which is explained by increasing the number of the foci pairs involved in the location

procedure. Again, the location errors slightly increase after adding random noise.

Finally, the influence of the velocity mismodelling is checked similarly to the ME method by calculating

Fig. 6 The variation of the average error of the double-difference locations: error in distance (*top*) and in the travel time RMS (*bottom*) with respect to the total number of event pairs and parameter MAXSEP (*data point labels*) for noise-free travel times (*solid lines*) and noisy travel times (*dashed lines*). The noise level is ± 15 ms for the P waves and ± 30 ms for the S waves



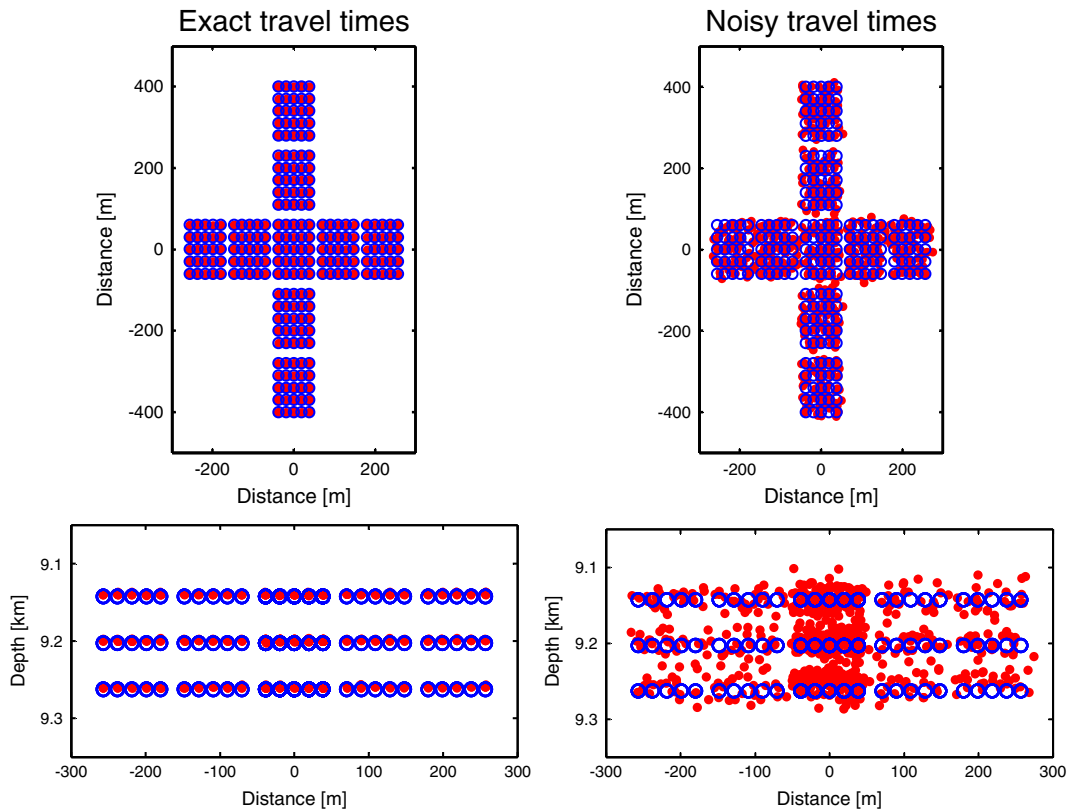


Fig. 7 Double-difference synthetic locations (*red dots*) with parameter MAXSEP of 1 km for noise-free travel times (*left*) and for noisy travel times (*right*) compared to the exact locations (*blue circles*). The noise level is ± 15 ms for the P waves and ± 30 ms for the S waves

the synthetic travel times in the 1D velocity model and locating in the homogeneous half-space velocity model. We examine the dependence of the location errors on distance from the centre of the foci cluster (Fig. 3). For noise-free data, the average location error is about 4.25 m, which is significantly smaller than the average error of the ME locations. Besides, no linear increase of the location error with distance from the centre of the cluster was found. Nevertheless, some foci with distance from the centre of the cluster larger than 300 m have larger errors (Fig. 3). The reason is that these foci are less linked to the others forming thus a smaller number of foci pairs.

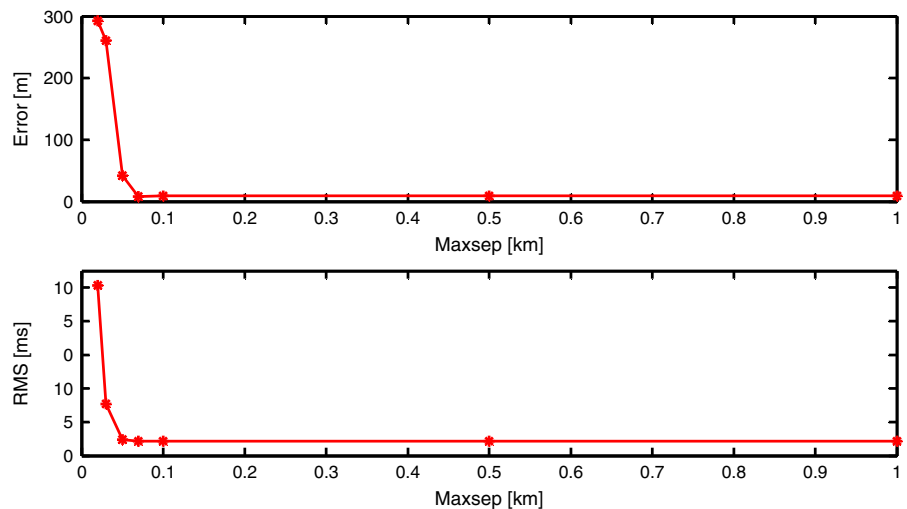
Note that in the case of the velocity mismodelling, a high value of MAXSEP can increase the error of the location and time. To examine this effect, we relocate the hypocentres in the inaccurate velocity model (homogeneous model) with varying MAXSEP. Figure 8 shows that the best accuracy is obtained for MAXSEP of 70 m with the average location error of 8.84 m. For MAXSEP of 1 km, the error reaches 9.36 m. This

means that the choice of the MAXSEP depends also on uncertainties in the velocity model, but this dependence seems to be rather weak.

3.3 Discussion

In order to compute highly precise locations, it is necessary to analyse the data and optimize the control parameters required in the ME and DD methods. In the case of the ME method, the precision of the location is mainly controlled by the choice of the master event. Its position must be accurately located to get the best absolute locations of foci. The relative position of the master event within the focal zone becomes important in the case of the velocity mismodelling. The most precise locations are obtained when the master event is positioned in the centre of the focal zone and the worst precise locations when the master event is positioned at the edge of the focal zone. Obviously, if the master event moves away from the middle of the zone, some events can be quite distant from the master

Fig. 8 The variation of the average error of the double-difference locations calculated for the homogeneous velocity model: distance (*top*) and the travel time RMS (*bottom*) with respect to the parameter MAXSEP. Noise-free travel times are used



event, and the location error becomes strongly influenced by the velocity mismodelling.

The DD method produces the most precise locations if the maximum separation distance (MAXSEP) is sufficiently large and allows for creating a sufficiently high number of foci pairs. In this case, the foci are strongly linked, and the inversion is well over-determined and stable. However, a high number of foci pairs cause the location procedure to be time consuming. For example, the computation can take several hours for three million foci pairs computed by an ordinary PC (2 GB RAM and 2.40 GHz processor frequency). Moreover, as shown for the velocity mismodelling, the choice of too large MAXSEP distance can be inadequate for the location (Fig. 8). Therefore, it is desirable to find an optimum value of MAXSEP which produces the best results for the given configuration.

The same synthetic tests (velocity mismodelling, noisy travel times and variable number of stations) were performed for both methods and revealed that the DD method yields more precise locations than the ME method. This is because all events interact between themselves in the DD method, while just one event interacts with the others in the ME method. The synthetic tests for the ME and DD methods also prove that there is no visible distortion of the focal zone, such as an artificial clustering of foci, in the relative locations under study. Artificial clustering does not appear even if the location accuracy is low or the velocity model is very approximate. This means that the clustering of

the ME or DD locations, when real datasets are processed, can be considered in most cases as reliable and not a numerical artefact of the location method. An exception might be configurations of a very low number of stations with poor azimuthal coverage and the velocity model characterized by extremely strong 3D inhomogeneities.

4 Application to the 2008 West Bohemia earthquake swarm

In this section, the precision and efficiency of the ME and DD location methods are exemplified on observations of the 2008 swarm activity in West Bohemia, Czech Republic. This area is known for its pertinent seismicity which is characterized by a frequent occurrence of earthquake swarms. The seismic activity in this region is one of the manifestations of the recent geodynamic activity displayed also by young Quaternary volcanism and ubiquitous emanations of mantle-derived carbon dioxide. One of the strongest recent earthquake swarms occurred in October 2008 (Fischer et al. 2010, Vavryčuk 2011a, b). This swarm lasted for 4 weeks and involved more than 25,000 micro-earthquakes with magnitudes higher than -0.5 . The magnitude of the strongest earthquake was 3.8. The hypocentres formed a 4-km long focal zone striking $N170^{\circ}E$ at depths of 7.5–10 km. The tectonic structure of the area is characterized by two main fault systems (Babuška et al. 2007): the Sudeten NW–SE fault system and the Ore Mountains (Eger Rift) WSW–ENE fault

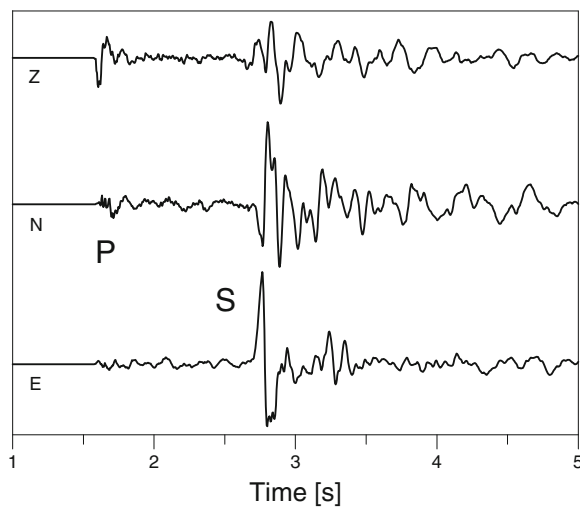
system. The tectonic complexity of the area is manifested by the existence of other minor fault systems (Bankwitz et al. 2003; Peterek et al. 2011).

4.1 Data

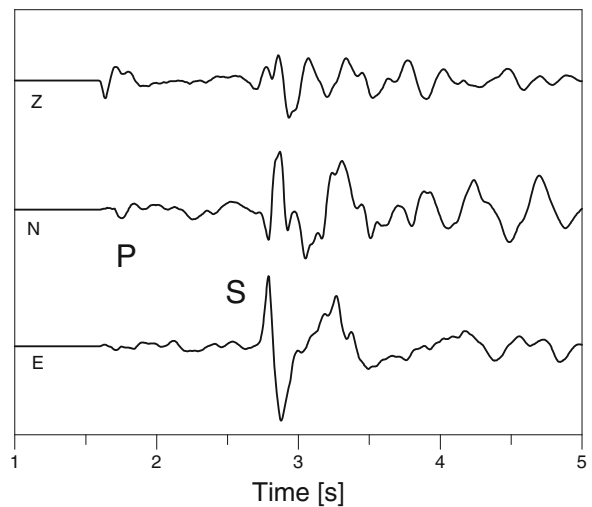
The analysed dataset consists of the P and S wave arrival times of 483 micro-earthquakes recorded at 23 local seismic stations of the WEBNET network (see Fig. 1). The sampling frequency is 250 Hz, and the error of manually picked arrival times is about ± 4 ms for the P waves and ± 10 ms for the S waves (Fig. 9). In addition to the absolute arrival times, we measured also the

waveform cross-correlation differential times. Thanks to the good quality of the manually picking time and short duration of the direct P wave pulse, a short time window was applied to observed waveforms before cross-correlations: 0.1 s before and 0.2 s after the manually picked P wave arrival times, and 0.1 s before and 0.3 s after the manually picked S wave arrival times. The differential times were obtained by cross-correlating waveforms in the frequency range from 3 to 10 Hz (Fig. 10). The reliability of the cross-correlation times was assessed by evaluating the correlation coefficient (Fig. 11) between the waveforms, only data with correlation coefficients higher than 0.8 being considered.

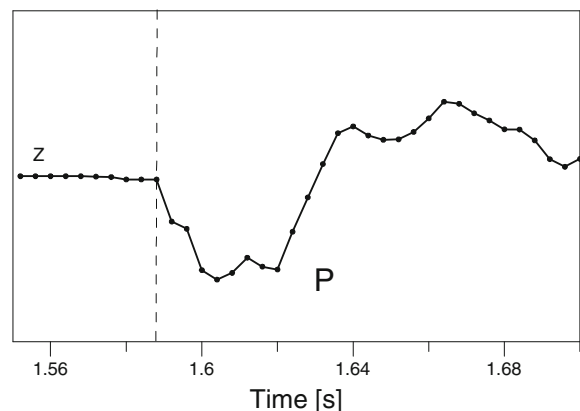
Velocity



Displacement



P-wave velocity



S-wave velocity

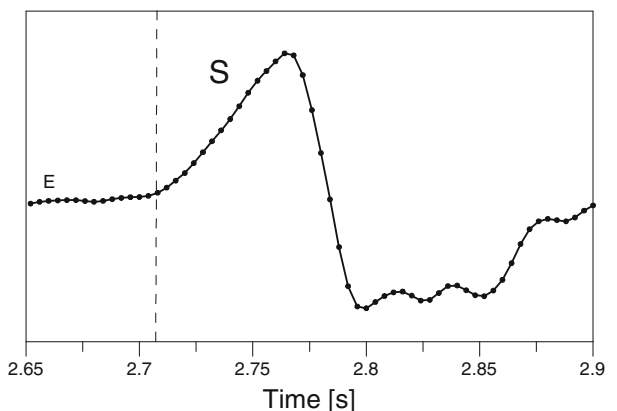


Fig. 9 Three-component velocity (*top left*) and displacement (*top right*) records of M 3.7 earthquake of 4 October 2008 at 19:00:33 (event ID: X5848A). *Bottom plots*: detailed waveforms of the vertical component of the P wave (*left*) and of E-

W component of the S wave (*right*) velocity. The *dashed line* shows the arrival times of the P and S direct waves; *dots* mark individual samples. The sampling interval is 4 ms. The records of the NKC station are displayed

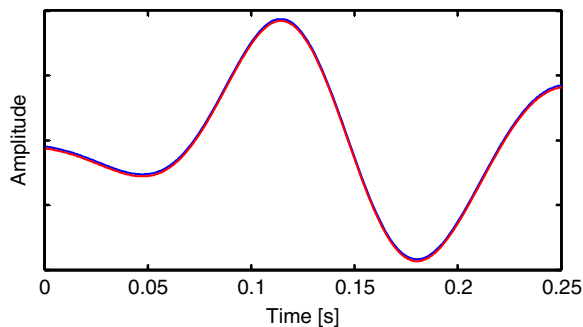


Fig. 10 P waveforms of two earthquakes normalized and shifted in time and overlaid after cross-correlation. *Blue line*: earthquake of 2008 October 9 at 22:57:38.250 (event ID: X1642A), $ML=1.4$. *Red line*: earthquake of 2008 October 9 at 22:09:12.320 (event ID: X1580A), $ML=1.4$. The P waveforms are band-pass filtered in the frequency range of 3 to 10 Hz, and a short time window is applied before the cross-correlation. The cross-correlation coefficient is 0.99. The records of the KVC station are displayed

Ultimately, 65,451 P wave and 60,660 S wave cross-correlation differential times were retained. The absolute delay time is computed by adding the differential time computed from the cross-correlation to the difference between the original times of the correlated waveforms.

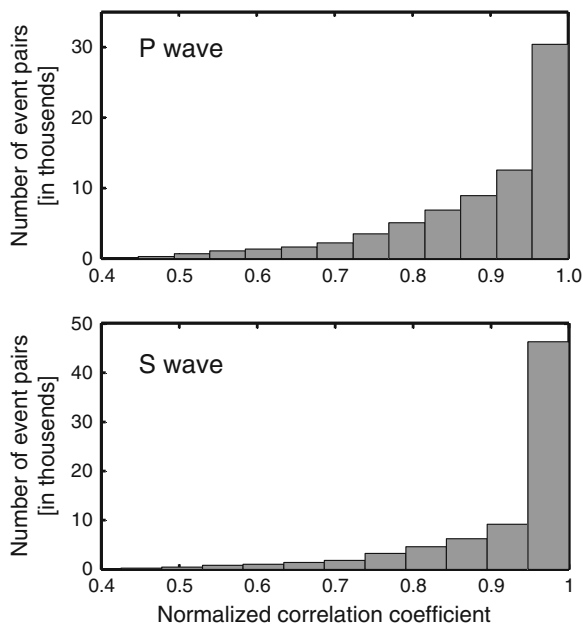


Fig. 11 Histograms of the cross-correlation coefficients of the P (*top*) and S waveforms (*bottom*) for all event pairs

4.2 Location strategy and control parameters

The initial hypocentre locations were determined using the location code FASTHYPO (Herrmann 1979) based on minimizing the travel time residuals at all stations for each event (Fig. 12). The same velocity model was used as in the synthetic tests (see Table 2). This model was obtained by refining the model of Málek et al. (2000) using the arrival times of local quarry blasts and micro-earthquakes, and it is considered as the optimum model for the region. The model is used in the initial locations as well as in relocations. The ratio V_p/V_s is equal to 1.70, and the uncertainties of the model should be less than 5%.

In the ME method, we chose the master event near the centre of the focal area. Given the high density of foci and the small and compact area of seismicity, just one master event is considered for the relocation. In the DD method, the maximum separation distance (MAXSEP) is chosen to be 0.7 km. This value is based on synthetic tests and ensures including a sufficiently high number of foci pairs and strong linking between the foci. Each hypocentre is connected to a minimum of ten other neighbours. During the relocation, we combine the catalogue times (CT) and the waveform cross-correlation differential times (CC) using the weighting scheme shown in Table 3 found by extensive testing of various schemes. In the first ten iterations, we down-weight the P wave and S wave CC data to 0.01, in order to allow for a coarse relocation. During the last ten iterations, both the P and S catalogue manually picked data are equally down-weighted to 0.01, in order to refine the relocation. A total of 30 iterations was performed. Since the tenth iteration, the observations with travel time residuals higher than 30 ms were down-weighted. A damping scheme was applied in the HypoDD code to control the stability of the least-squares inversion, which is quantified by the condition number. We get a condition number equal to 65 at the last iteration, which is in the range between 40 and 80 recommended for the stable inversion (Waldhauser 2001).

4.3 Results

Figure 13 shows the relocation of the 2008 swarm for the three methods: master event (ME), DD using the catalogue times (DD-CT) and also the cross-correlation delay times (DD-CC). All three methods display a

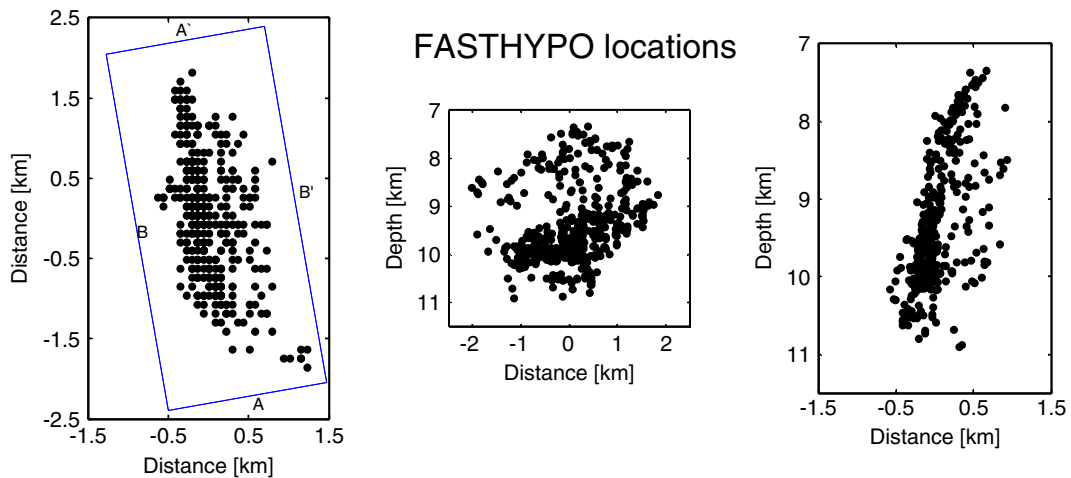


Fig. 12 Locations of the 2008 earthquake swarm using the FASTHYPO code (Herrmann 1979). *Left*: map view; *middle*: along-strike (section parallel to *B*); *right*: across-strike (section parallel to *A*). The origin of coordinates represents the centre of

the cluster with latitude=50.216°, longitude=12.448° and depth =9.197 km. The location errors are about 200 m in the epicentre position and 350 in depth

significant improvement in precision when compared to the initial locations computed by the FASTHYPO code (Fig. 12). This is because the systematic errors due to the station effects and the inaccurate velocity model between the source and stations are well compensated, thanks to the dense distribution of foci in the focal zone area and a carefully selected master event. Among the three methods, the ME locations display the lowest precision. The DD method using the catalogue data (DD-CT locations) performs better, and the highest precision is achieved when the waveform cross-correlation differential times (DD-CC locations) are included which results in the lowest dispersion of seismicity.

The map view and the cross sections of the final locations in Fig. 13 show that the foci roughly cover

an area of 2×4 km within a depth range of 7–11 km. The fault shows a complicated geometry consisting of several segments with different orientations. The majority of events occurred in the main part of the fault zone located between depths of 8.3 and 10.3 km. The map view projection shows that this fault segment is striking 169° from the north and dipping 80° from the vertical. The deeper part of the fault, between depths of 10.3 and 11 km, shows a different orientation compared to the main fault segment, displayed in the cross-section projection (parallel to *BB'*). The same section shows that the upper part of the fault, located between depths of 7.2 and 9 km, has a remarkably different dip (68°) compared to the main fault segment.

Table 2 The West Bohemia velocity model

Layer number	Depth (km)	P wave velocity (km/s)
1	0.0	4.30
2	0.2	5.06
3	0.5	5.33
4	1.0	5.60
5	2.0	5.87
6	4.0	6.09
7	6.0	6.35
8	10.0	6.74
9	20.0	7.05
10	32.0	7.25

Table 3 Weighting scheme

Iteration	WTC CP	WTC CS	WRCC (s)	WTC TP	WTC TS	WRCT (s)
10	0.01	0.01	NAN	1	0.75	NAN
10	0.01	0.01	NAN	1	0.75	0.03
5	1	1	NAN	0.01	0.01	0.03
5	1	1	0.015	0.01	0.01	0.03

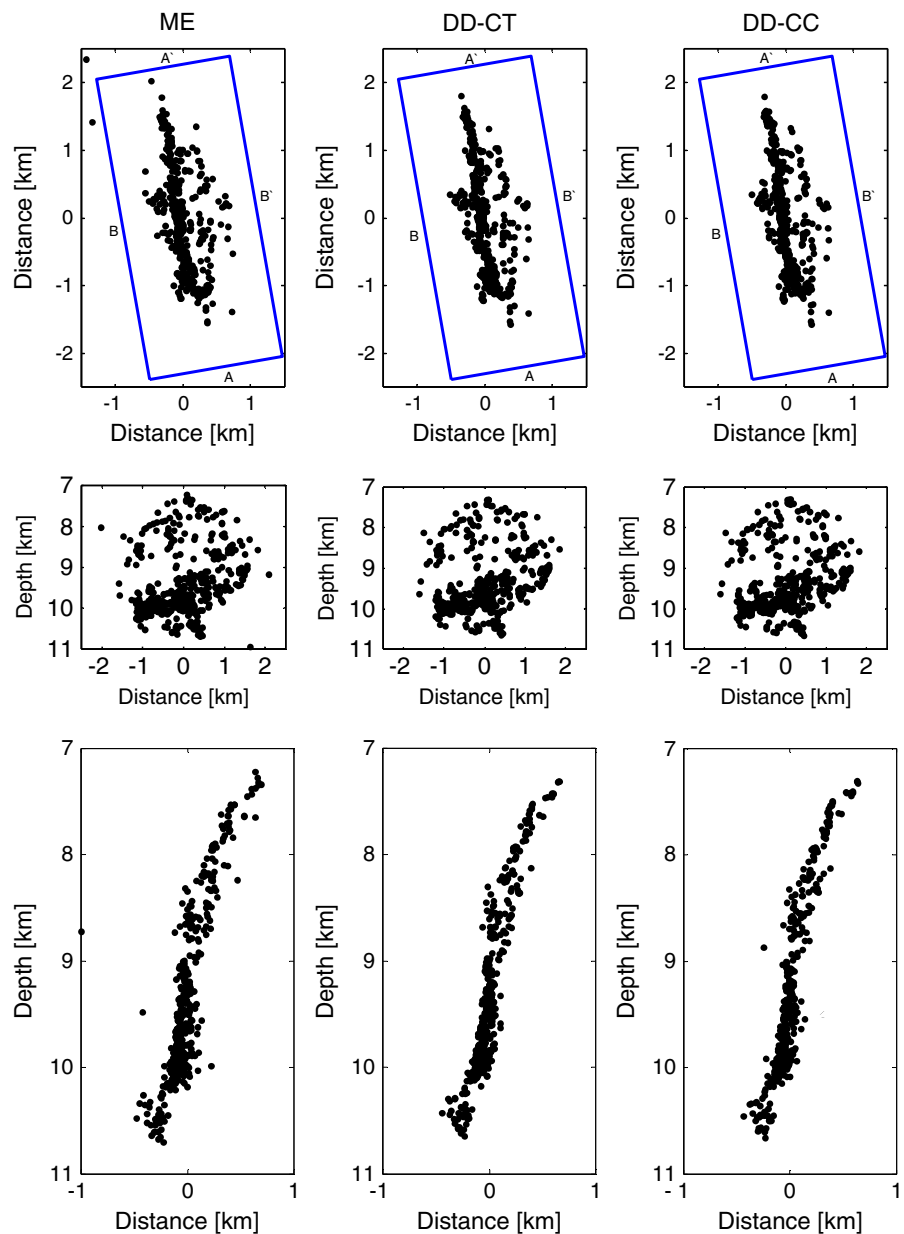
WTCCP and WTCCS are the weighting parameters for the cross-correlation differential times of the P and S waves, respectively. WTCTP and WTCTS are the weighting parameters for the catalogue differential times of the P and S waves, respectively. WRCC and WRCT are the RMS weighting for the cross-correlated and catalogue differential times. The symbol NAN means that the weight is not considered in the computation

We assessed the location errors of the ME and DD methods by relocating foci with the use of noisy travel times with random noise in the range of estimated picking errors for the West Bohemia data (± 4 ms for the P waves and ± 8 ms for the S waves). The location error is then estimated as the difference between the locations using the noise-free and noisy data. Figure 14 shows that the lowest error was achieved by the DD-CC method (i.e. using the cross-correlation times). The average location error is 17 m, and the

average RMS is 4.8 ms. The error of the ME method is about 62 m in location and 12.6 ms in the RMS.

We estimated also the errors induced by uncertainties of the velocity model by perturbing the velocity in all layers by ± 5 %. If we apply the DD-CC method (i.e. using the cross-correlation times), the average location error is 105 m for the slow velocity model and 94 m for the fast velocity model. As shown in Fig. 15, the velocity model uncertainties cause a slight shift in the fault position but do not change its shape and orientation.

Fig. 13 Locations of the 2008 earthquake swarm using the master-event method (ME), double-difference method with catalogue data only (DD-CT) and with both catalogue and waveform cross-correlation data (DD-CC). *Top row*: map view; *middle row*: along-strike (section parallel to *B*); *bottom row*: across-strike (section parallel to *A*)



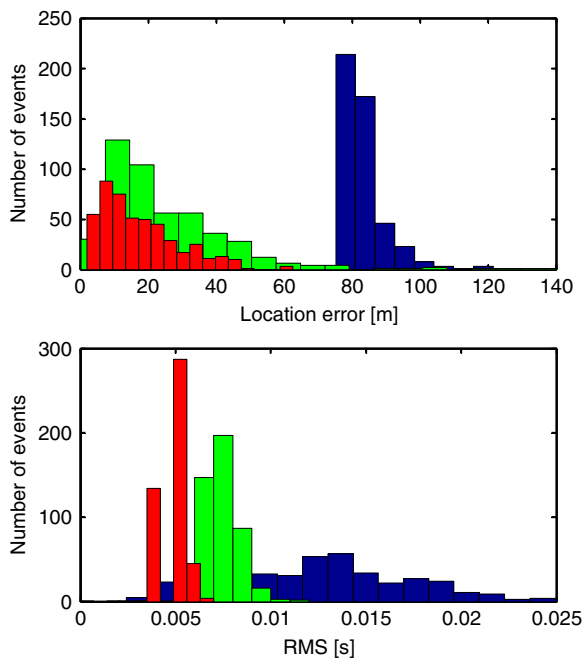


Fig. 14 Errors of locations (*top*) and travel time RMS (*bottom*) determined for the master-event method (*blue*), the double-difference method using catalogue data (*green*) and the double-difference method using both catalogue and waveform cross-correlation data (*red*). The errors in locations are estimated by perturbing the arrival time by random noise with noise level ± 4 ms for the P waves and ± 8 ms for the S waves

Similar results are obtained also when the P-to-S velocity ratio is perturbed.

The synthetic tests have confirmed (Fig. 3) that the errors of the ME locations increase with distance from the master event, which is most probably caused by the higher sensitivity of the ME method to the uncertainties in the velocity model and to unknown velocity variations in the focal zone. In real data, the errors of the ME method, estimated as the differences between the ME and DD-CC locations, also slightly increase with distance of the foci from the position of the master event (see Fig. 16). This confirms that the DD method is more suitable for locating earthquake clusters with larger dimensions.

5 Double-difference locations of the 1993–2011 swarm activity in the main focal zone of West Bohemia

As mentioned in the previous sections, the DD method outperforms the ME location mainly in the ability to

relocate large heterogeneous data sets. This property is particularly advantageous when analysing seismicity covering a long time period during which the seismic network could experience several reconfigurations and/or temporary station breakdowns. As a result, long-term observations of seismicity are usually of variable quality, and a unified, detailed and accurate seismicity image is difficult to obtain.

In this section, we employ the robustness of the DD location method on analysing the seismic activity within the fault zone of Nový Kostel in West Bohemia where the most intense swarms took place during the past 20 years (Fischer and Horálek 2003; Fischer and Michálek 2008; Hiemer et al. 2012). Due to a large number of waveforms and high quality of the manually picked absolute arrival times, only the catalogue differential times are used in the relocation. The main control parameters of the relocation were as follows: we used a minimum of four stations per event, a minimum of four neighbouring events, the MAXSEP parameter was 300 m, weights were 1 for the P waves and 0.75 for the S waves, and we performed 30 iterations with damping of 120.

Figure 17 shows that the hypocentres in the focal zone of Nový Kostel cover roughly an area of 7×8 km and are within a depth range of 6–13 km. The fault areas activated by swarms in 2000 and 2008 overlap and show a high density of foci. The DD locations prove that the fault surfaces of the 2000 and 2008 swarms are identical within the range of the location error. An analysis of the Coulomb stress changes indicates that the 2008 swarm occurred partly as a reactivation of the 2000 swarm fault patch (Hainzl et al. 2012). Interestingly, the 2011 swarm has activated a new fault segment adjacent to the north. While the upper part of the 2011 fault patch at depths smaller than about 8 km aligns with the fault patch of the 2000 and 2008 swarms dipping west, the lower part dips in the opposite direction, to the east. This confirms that the complicated geometry of the fault of the 2008 swarm as shown in Section 4.3 is even more pronounced on a larger scale of the fault zone. The DD locations of the 2011 swarm presented here are not complete because of the ongoing manual processing of the swarm events.

6 Conclusions

The synthetic tests proved that the ME and DD location methods are powerful tools capable of retrieving

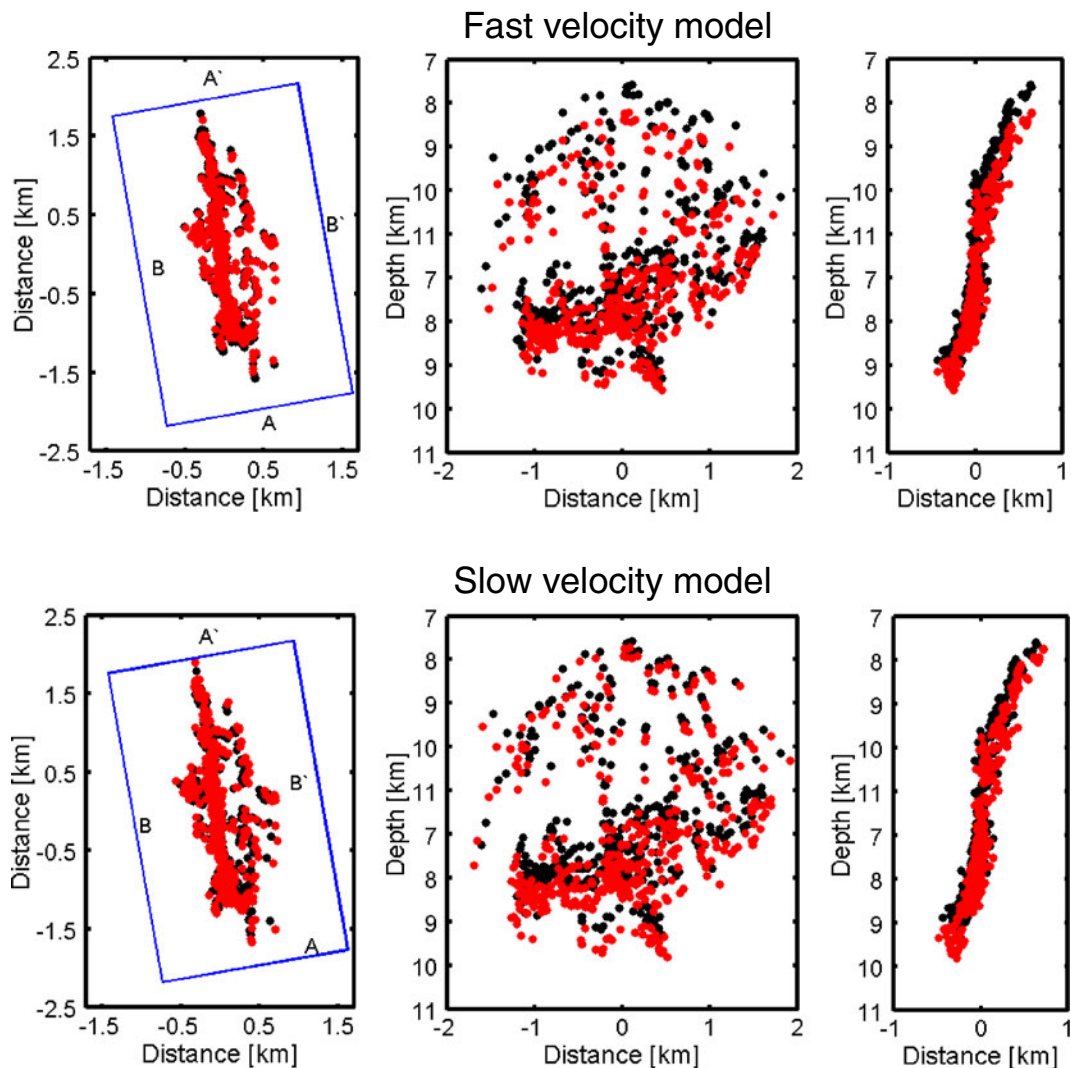


Fig. 15 The double-difference locations using the waveform cross-correlation data (DD-CC) calculated for the exact (*black*) and perturbed (*red*) velocity models. The perturbed velocity

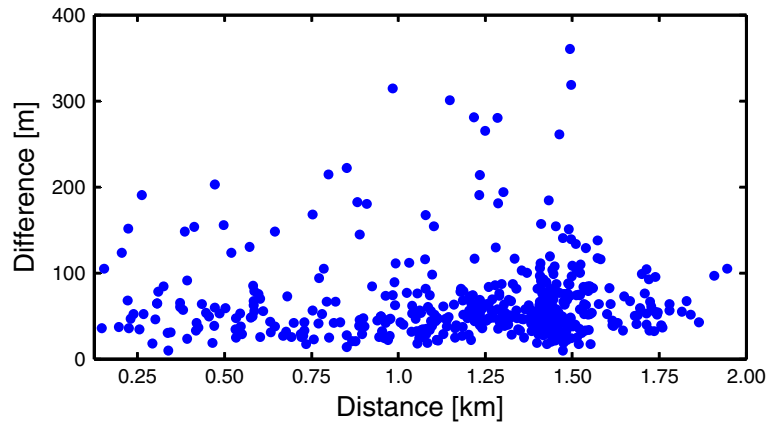
models are obtained by increasing (*top*) and decreasing (*bottom*) the velocity by 5 % of the exact velocity

details of the fault geometry. As regards location precision and robustness with respect to errors in arrival times and inaccuracies in the velocity model, the DD method performs better than the ME method. The DD locations of the synthetic data are twice as accurate as the ME locations. The precision of the DD method may be further improved by including the waveform cross-correlation differential times. The ME method is also highly precise but yields less stable results being sensitive to the selection of the master event. This limits its application to smaller earthquake clusters so that the ray paths from foci to the individual stations

could be regarded parallel. Importantly, both ME and DD locations display no visible distortion of the foci zone and no artificial clustering of foci even in case of noisy travel times.

The application of the ME and DD methods to observations of the 2008 earthquake swarm in West Bohemia, Czech Republic, reveals that both methods perform significantly better than the standard absolute locations. The estimated relative location errors range from 17 m for the DD-CC method to 62 m for the ME method. The higher precision of the DD method is pronounced also in the more focused image of the

Fig. 16 The difference between the master-event and double-difference locations using the cross-correlation differential times



complicated fault geometry. The fault zone is segmented to sub-faults which show different orientations. This points to the significance of precise

locations of foci, which can help in reconstructing a detailed fault structure and in understanding complex physical processes in the focal area.

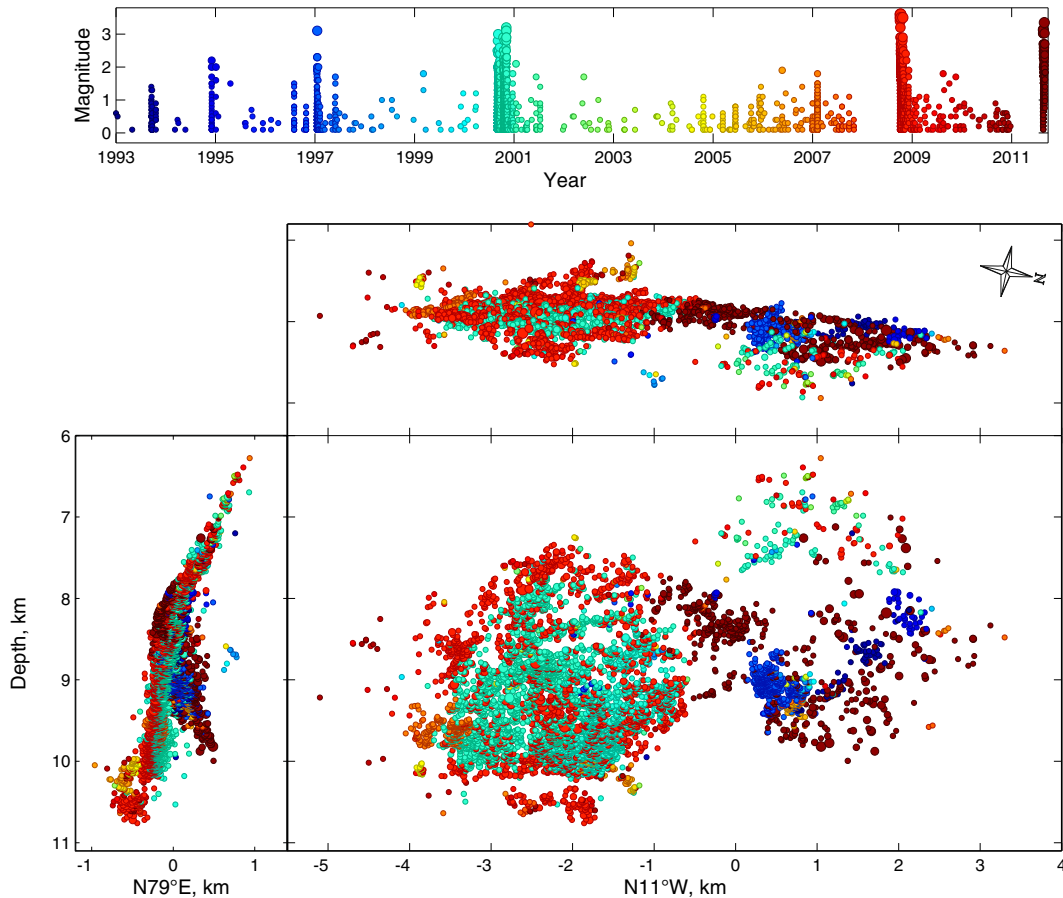


Fig. 17 Hypocentres of the seismic activity in the Nový Kostel fault zone for the period from 1993 to 2011 relocated by the double-difference method. Magnitude–time plot (*top*) and locations (*bottom*). The locations are shown in the map view (*upper*

part) and in two vertical cross-sections (*lower part*) along profiles AA' and BB' indicated in Fig. 13. Note that above the depth 8.3 km, all the activity aligns along a common steeply dipping fault plane. The hypocentres are *colour-coded* by origin time

Finally, we presented the DD locations of the seismic activity in the focal zone of Nový Kostel in West Bohemia in the period from 1993 to 2011. In this period, several major earthquake swarms occurred and activated various differently oriented fault zones composed of a number of fault patches with a prevailing NNW–SSE orientation. While the 2000 and 2008 earthquake swarms shared a common fault plane, the 2011 swarm extends the activated area by 4 km to the north.

Acknowledgments We thank two anonymous reviewers for their helpful reviews, Alena Boušková, Josef Horálek and other colleagues from the WEBNET group for providing us with the data from the 2008 swarm activity and for their kind help with pre-processing them, and Pavla Hrubcová for many lively discussions of the subject. The work was supported by the Grant Agency of the Academy of Sciences of the Czech Republic, Grant IAA300120905, by the Grant Agency of the Czech Republic, Grant P210/12/1491, by the Czech Ministry of Education Research Plan, Grant MSM0021620855, by project CzechGeo, Grant LM2010008, and by the European Community's FP7 Consortium Project AIM “Advanced Industrial Microseismic Monitoring”, Grant Agreement 230669.

References

- Andrews V, Stock J, Ramírez-Vázquez CA, Reyes-Dávila G (2011) Double-difference relocation of the aftershocks of the Tecmán, Colima, Mexico earthquake of 22 January 2003. *Pure Appl Geophys* 168(8–9):1331–1338
- Babuška V, Plomerová J, Fischer T (2007) Intraplate seismicity in the western Bohemian Massif (central Europe): a possible correlation with a paleoplate junction. *J Geodyn* 44(3–5):146–159
- Bankwitz P, Schneider G, Kämpf H, Bankwitz E (2003) Structural characteristics of epicentral areas in Central Europe: study case Cheb Basin (Czech Republic). *J Geodyn* 35(1–2):5–32
- Bulut F, Aktar M (2007) Accurate relocation of Izmit earthquake (Mw=7.4, 1999) aftershocks in Cinarcik Basin using double difference method. *Geophys Res Lett* 34(10):L10307
- Deichmann N, Garcia-Fernandez M (1992) Rupture geometry from high-precision relative hypocenter locations of micro-earthquake clusters. *Geophys J Int* 110(3):501–517
- Fischer T, Horálek J (2003) Space-time distribution of earthquake swarms in the principal focal zone of the NW Bohemia/Vogtland seismoactive region: period 1985–2001. *J Geodyn* 35(1–2):125–144
- Fischer T, Michálek J (2008) Post 2000-swarm microearthquake activity in the principal focal zone of West Bohemia/Vogtland: space-time distribution and waveform similarity analysis. *Stud Geophys Geod* 52:493–511
- Fischer T, Horálek J, Michálek J, Boušková A (2010) The 2008 West Bohemia earthquake swarm in the light of the WEBNET network. *J Seismol* 14:665–682. doi:10.1007/s10950-010-9189-4
- Fréchet J (1985) *Sismogenese et doublets sismiques, these d'etat*, Universite scientifique et Medicale de Grenoble, France
- Gibowicz SJ, Kijko A (1994) *An introduction to mining seismology*. Academic, San Diego
- Got JL, Fréchet J, Klein FW (1994) Deep fault plane geometry inferred from multiplet relative relocation beneath the south flank of Kilauea. *J Geophys Res* 99(B8):15375–15386
- Hainzl S, Fischer T, Dahm T (2012) Seismicity-based estimation of the driving fluid pressure in the case of swarm activity in Western Bohemia. *Geophys J Int* 191:271–281. doi:10.1111/j.1365-246X.2012.05610.x
- Havskov J, Ottemoller L (2010) *Routine data processing in earthquake seismology*. Springer, Dordrecht
- Herrmann RB (1979) FASTHYPO—a hypocenter location program. *Earthq Notes* 50(2)
- Hiemer S, Rößler D, Scherbaum F (2012) Monitoring the West Bohemian earthquake swarm in 2008/2009 by a temporary small-aperture seismic array. *J Seismol* 16(2):169–182. doi:10.1007/s10950-011-9256-5
- Jones GA, Nippres SEJ, Rietbrock A, Reyes-Montes JM (2008) Accurate location of synthetic acoustic emissions and location sensitivity to relocation methods, velocity perturbations, and seismic anisotropy. *Pure Appl Geophys* 165(2):235–254
- Jordan TH, Sverdrup KA (1981) Teleseismic location techniques and their application to earthquake clusters in the south-central Pacific. *Bull Seismol Soc Am* 71(4):1105–1130
- Lay T, Wallace T (1995) *Modern global seismology*. Academic, San Diego
- Lin GQ, Shearer P (2005) Tests of relative location techniques using synthetic data. *J Geophys Res* 110:B04304. doi:10.1029/2004JB003380
- Málek J, Janský J, Horálek J (2000) Layered velocity models of the western Bohemia region. *Stud Geophys Geod* 44(4):475–490
- Menke W (1989) *Geophysical data analysis: discrete inverse theory*. Academic, San Diego
- Menke W, Schaff D (2004) Absolute earthquake locations with differential data. *Bull Seismol Soc Am* 94(6):2254–2264
- Michelini A, Lomax A (2004) The effect of velocity structure errors on double-difference earthquake location. *Geophys Res Lett* 31(9):L09602. doi:10.1029/2004GL019682
- Pavlis GL (1986) Appraising earthquake hypocenter location errors—a complete, practical approach for single-event locations. *Bull Seismol Soc Am* 76:1699–1717
- Peterek A, Reuther CD, Schunk R (2011) Neotectonic evolution of the Cheb Basin (Northwestern Bohemia, Czech Republic) and its implications for the late Pliocene to Recent crustal deformation in the western part of the Eger Rift. *Z Geol Wiss Berlin* 39(5/6):335–365
- Richards-Dinger KB, Shearer PM (2000) Earthquake locations in southern California obtained using source-specific station terms. *J Geophys Res* 105:10939–10960

- Stoddard PR, Woods MT (1990) Master event relocation of Gorda Block earthquakes—implications for deformation. *Geophys Res Lett* 17(7):961–964
- Vavryčuk V (2011a) Principal earthquakes: theory and observations from the 2008 West Bohemia swarm. *Earth Planet Sci Lett* 305:290–296. doi:[10.1016/j.epsl.2011.03.002](https://doi.org/10.1016/j.epsl.2011.03.002)
- Vavryčuk V (2011b) Detection of high-frequency tensile vibrations of a fault during shear rupturing: observations from the 2008 West Bohemia swarm. *Geophys J Int* 186:1404–1414. doi:[10.1111/j.1365-246X.2011.05122.x](https://doi.org/10.1111/j.1365-246X.2011.05122.x)
- Waldhauser F (2001) HypoDD—a program to compute double difference hypocenter locations (HypoDD version 1.0—03/2001). Open File Report, US Geological Survey, Menlo Park, pp. 01–113
- Waldhauser F, Ellsworth WL (2000) A double-difference earthquake location algorithm: method and application to the northern Hayward fault, California. *Bull Seismol Soc Am* 90:1353–1368
- Waldhauser F, Ellsworth WL (2002) Fault structure and mechanics of the Hayward Fault, California, from double-difference earthquake locations. *J Geophys Res* 107: B32054. doi:[10.1029/2000JB000084](https://doi.org/10.1029/2000JB000084)
- Zollo A, De Matteis R, Capuano P, Ferulano F, Iannaccone G (1995) Constraints on the shallow crustal model of the Northern Apennines (Italy) from the analysis of micro-earthquake seismic records. *Geophys J Int* 120:646–662